Carbohydrate Polymers 83 (2011) 1723–1729

Contents lists available at ScienceDirect

Carbohydrate Polymers

journal homepage: www.elsevier.com/locate/carbpol

Controlled synthesis of amphiphilic rod-coil biodegradable maltoheptaose-graft-poly(ε-caprolactone) copolymers

Qiu Xiongying, Wang Caiqi*, Shen Juan, Jiang Mingwei

College of Chemistry and Chemical Engineering, Graduate University of the Chinese Academy of Sciences, 19A Yuquan Road, Beijing 100049, PR China

ARTICLE INFO

Article history:
Received 29 March 2010
Received in revised form 2 October 2010
Accepted 19 October 2010
Available online 23 October 2010

Keywords:
Graft copolymer
Maltoheptaose
Biodegradable
Amphiphilic
Rod-coil

ABSTRACT

The controlled synthesis of novel amphiphilic biodegradable maltoheptaose-graft-poly(ε-caprolactone) copolymers was achieved through a three-step method. The first step consisted of partial silylation of the maltoheptaose hydroxyl groups. This protection step was followed by ring-opening polymerization of ε-caprolactone initiated from the remaining OH functional group of the partially silylated oligosaccharide. The third step involved the deprotection of the silylether group under mild conditions. The effects of varying the experimental conditions on grafting efficiency and graft length were investigated to ensure controlled polymerization of ε-caprolactone. The protection and deprotection of the TMS group during the entire procedure were carefully monitored with Fourier transform infrared (FTIR) and ^{1}H NMR. The final graft copolymers were characterized by FTIR, ^{1}H NMR, gel permeation chromatography (GPC), and differential scanning calorimetry (DSC).

1. Introduction

Interest in the study of amphiphilic biodegradable copolymers has increased due to their controlled biodegradation rates and potential applications in drug delivery and separation technologies (Nie, Zhao, Xie, & Wu, 2003; Ouchi, Kontani, & Ohya, 2003; Rosler, Vandermeulen, & Klok, 2001). At present, amphiphilic linear copolymers have been extensively studied (Caillol et al., 2003; Chang, Bender, Phelps, & Allcock, 2002; Luo et al., 2004; Nie, Zhao, Xie, & Wu, 2003; Xiong, Tam, & Gan, 2003). In contrast, relatively few works have been done on amphiphllic non-linear copolymers such as graft copolymers (Jeong, Kang, Yang, & Kim, 2002; Li, Zhu, Sunintaboon, & Harris, 2002) despite the numerous advantages of providing integrations of considerable functionality onto the polymer backbone (Breitenkamp, & Emrick, 2003; Sato et al., 2005).

Recently, saccharide-based graft copolymers have attracted much attention not only because of their potential in separation technologies and controlled drug release but also because they serve as possible alternatives to existing non-biodegradable formulated systems (Hua, Jianga, Dinga, Gea, Yuanb, Yanga, 2002; Liu, Tian, & Hu, 2004; Nouvel, Frochot, Sadtler, Dubois, Dellacherie & Six, 2004a; Tatsuro, Tomohiro, & Yuichi, 2003). Especially, the protection and deprotection of partial hydroxyl groups via trimethylsilyl (TMS) groups have been successfully used in the preparation of polysaccharide-based graft copolymers with controlled structures in a homogeneous system (Nouvel et al., 2004a; Nouvel, Dubois, Dellacherie, & Six, 2004b; Ohya, Maruhashi, & Ouchi, 1998; Ouchi et al., 2003; Ydens, Rutot, Degee, Six, Dellacherie, & Dubois, 2000). For example, Ohya and Nouvel synthesized pollulan-g-poly(lactic acid) and dextran-g-poly(lactic acid) via ring-opening graft polymerization of lactide onto the corresponding trimethylsilyl (TMS) protected polysaccharides followed by the removal of TMS protection groups. In this regard, we have also synthesized hydroxylpropyl cellulose-g-poly(ε-caprolactone) with controlled structures (Wang, Dong, & Tan, 2003).

Most saccharide-based surfactants are based on polysaccharides, so studies on the synthesis of saccharide-based graft copolymers mostly focus on the traditional comb-shaped or brush-shaped graft copolymers based on longer main chains as backbone ($M_n \approx 10{,}000 \sim$ several ten thousands) and shorter side chains as graft segments (Nouvel et al., 2004a,b; Ydens et al., 2000; Ohya et al., 1998; Ouchi et al., 2003; Liu et al., 2004; Yao et al., 2003). Only a few studies mention the use of oligosaccharides as precursors of macromolecular amphiphilic architectures. Recently, we reported the controlled synthesis of a new kind of amphiphilic graft copolymer based on a chitooligosaccharide (COS, M_n = 1500–2000, the degree of polymerization is about 11) as the hydrophilic short rigid backbone and poly(ε-caprolactone) (PCL) as the hydrophobic long side chain (Wang, Li, & Guo, 2005). The structure of this graft copolymer is different from the conventional comb-shaped or brush-shaped graft copolymers, and these special graft

* Corresponding author. Tel.: +86 10 88256677; fax: +86 10 88256092.
E-mail address: wang-caiqi@gucas.ac.cn (C. Wang).

0144-8617/$ – see front matter © 2010 Elsevier Ltd. All rights reserved.
doi:10.1016/j.carbpol.2010.10.034

copolymers COS-g-PCL can form multiple self-assembled morphologies.

In this study, maltoheptaose (MH, with a degree of polymerization of 7) which has a shorter saccharide chain and a narrower molecular distribution compared with chitooligosaccharide is chosen as the hydrophilic short rigid backbone and poly(ε-caprolactone) (PCL) as the hydrophobic long side chain. A new amphiphilic poly(ε-caprolactone) (PCL)-grafted maltoheptaose copolymer is synthesized by the protection and deprotection of partial hydroxyl groups via trimethylsilyl (TMS) groups. Further studies on the self-assembled morphologies of MH-g-PCL are still ongoing.

2. Experimental

2.1. Materials

β-cyclodextrin (β-CD) purchased from Beijing Solarbio Science & Technology Co., Ltd. (PR China) was recrystallized twice from water and vacuum-dried at 60 °C under vacuum before use. ε-caprolactone (Acros Organics, 99%) was dried over CaH_2 for 48 h, distilled under reduced pressure with the fraction collected at 96–98 °C (5 mmHg), and stored under inert atmosphere. Stannous octoate ($Sn(Oct)_2$) was purchased from Alfa-Aesar and used without any further purification. p-Xylene and THF were dried by refluxing over CaH_2 and Na/benzophenone complex and distilled just before use. DMSO was dried over 4 Å molecular sieves, distilled under reduced pressure, and stored under nitrogen atmosphere. Hydrochloric acid (36–38%), 1,1,1,3,3,3- hexamethyldisilazane (HMDS), and other regents were purchased from commercial sources and used as received without further purification.

2.2. Maltoheptaose from β-cyclodextrin

A total of 100 g of β-CD was dissolved in 600 ml of 0.01 M hydrochloric acid and kept under reflux for exactly 2 h (Volker, Gerd, & Reimund, 1995). The solution was neutralized with a calculated amount of 1 M NaOH (6 ml) and buffered to pH = 7.0 with Na_2HPO_4/NaH_2PO_4. The color changed to a pale yellow. The solution was stored at 4 °C for 12 h. A total of 85% of the educt crystallized from the solution. The regenerated cyclodextrin was filtered off and collected for the next run. The remaining solution was warmed up to 60 °C, saturated with p-xylene (approximately 1 ml), and stirred for several hours. Crystallization of cyclodextrin was completed by placing it in the refrigerator overnight. p-Xylene/cyclodextrin complex was removed from the solution by filtration, and water was removed under reduced pressure to l/10 of the initial volume. After further saturation with p-xylene, final traces of the cyclical educt were crystallized overnight at 4 °C and removed by filtration. Evaporation of the water under reduced pressure and drying in a vacuum resulted in crude maltoheptaose that was contaminated only by traces of oligoglucans ($Glcz_6$ up to $Glcs_2$) and sodium chloride/phosphate. The crop was dissolved in 40 ml of water and added dropwise to 1500 ml of ethanol. Pure precipitated maltoheptaose was removed by filtration and dried in a vacuum for several days with a yield of 10% maltoheptaose.

2.3. Preparation of maltoheptaose-g-PCL copolymers

2.3.1. Trimethylsilylation of maltoheptaose

Maltoheptaose was placed in a previously dried and nitrogen-purged round-bottom two-necked flask with a stopcock and connected to an oil valve for ammoniac evolution. After flushing with high-purity N_2 for 20 min, the desired amount of DMSO (10 wt % dried maltoheptaose) was added. Once maltoheptaose was totally dissolved, a predetermined amount of HMDS was added under nitrogen flow using previously dried syringes. The reaction medium was kept at the desired temperature for 3 h at a suitable stirring rate. The mixture was precipitated in deionized cool water after cooling slowly, and the product was washed thrice with cool water to remove unreacted maltoheptaose. The crude product was purified by repeated dissolution in acetone and precipitation in water, filtrated, and then dried for 72 h at 50 °C under vacuum. The trimethylsilyl substitution (D_{TMS}) of maltoheptaose was determined using the following equation:

$$D_{TMS} = \frac{7I_{Si(Me)_3}}{23 \times 9I_{H_1}} \times 100\% \quad (1)$$

where $I_{Si(Me)_3}$ and I_{H_1} are the integral areas of the signals for the methyl protons of the TMS groups at around $\delta = 0.1$ ppm and that for the methine protons (H-1) of the monosaccharide residue at around $\delta = 5.0$ ppm, respectively (Table 1).

IR (KBr, power, cm^{-1}): 3450 (O–H), 2960 (C–H), 2896 (C–H), 1250 (Si–CH_3), 1150–1000 (pyranose), 877, 843 (Si–CH_3), 752. ^1H NMR (600 MHz, D_2O or $CDCl_3$, δ, ppm): 5.3 (H-1 of pyranose), 5.1 (H-1′ of pyranose), 3.0–4.0 (H-2, -3, -4, -5, and -6 of pyranose), 0.1 (–O–Si(CH_3)$_3$)

2.3.2. ROP of CL from silylated maltoheptaose

The ROP of CL was performed in a previously dried two-necked round-bottom flask equipped with a stopcock and a rubber septum, purged with nitrogen. TMS-maltoheptaose (1.0 g) was dissolved in fresh, purified p-xylene (concentration ~20%), and a desired amount of the ε-caprolactone monomer and a drop of $Sn(Oct)_2$ were added under N_2. The mixture in a capped vial under N_2 was placed in a preheated oil bath at 110 °C and stirred for 24 h. Finally, TMS-maltoheptaose-g-PCL was recovered by precipitation in methanol, filtration, and drying under vacuum.

IR (KBr, power, cm^{-1}): 3440 (O–H), 2950 (C–H), 2896 (C–H), 1730 (C=O), 1251, 1150–1000 (pyranose), 877, 841, 753. ^1H NMR (600 MHz, $CDCl_3$, δ, ppm): 4.2–4.9 (H-1 of pyranose), 3.0–4.0 (H-2, -3, -4, -5, and -6 of pyranose), 3.9 (–CH_2–O–C (O)–), 2.5 (–O–C (O)–CH_2–), 1.5 (–O–C(O)–C–CH_2– and –CH_2–C–O–C (O)–), 1.2 (–C(O)–C–C–CH_2–C–C–O–), 0.1 (–O–Si(CH_3)$_3$).

2.3.3. Deprotection of TMS maltoheptaose-g-PCL

The protected graft copolymers were dissolved in THF (10 wt% PCL-grafted silylated maltoheptaose) along with the addition of a slight excess of HCl aqueous solution (0.1 M) with respect to the number of "–O–Si(CH_3)$_3$" functions. The deprotected copolymers were recovered by precipitation in cold water, filtration, and vacuum drying.

The average polymerization degree of ε-caprolactone grafted on every glucose unit of MH backbone (DP) was calculated from the ratio of the integral areas of the methylene protons signal of PCL at 2.2 ppm to the methine proton signal (H-1) of MH at 4.3 ppm (Table 2).

2.4. Measurements

^1H NMR analyses were carried out using a JOEL JNM-ECA600 spectrometer in $CDCl_3$, in DMSO-d_6, or in D_2O at room temperature (TMS-free solvents). FT-IR measurements were carried out on an AVATAR 360 FT-IR spectrometer (Thermo Nicolet). The samples for FT-IR analysis were prepared by dispersing the powder in KBr and compressing the mixtures to form disks. Molecular weight (M_n) and molecular weight distribution (M_w/M_n) were measured with a Viscotek TDA 302 GPC instrument with tetrahydrofuran (THF) as the mobile phase and polystyrene as calibration standard. The melting point (T_m) was measured by employing a differential scanning calorimeter (DSC-60 SHIMADZA, Japan). The samples were

Table 1
Characterization of β-CD, MH, and trimethylsilyed maltoheptaose.

Sample	DS[a] (%)	Solubility					
		DMSO[b]	Chloroform	Acetone	Petroleum ether	p-Xylene	Water
β-CD	0	+	–	–	–	–	–/+
MH	0	+	–	–	–	–	+
TMSMH-1	4.78	+	–	–	–	–	+
TMSMH-2	9.83	+	+	+	–	+	+
TMSMH-3	48.77	–	+	+	+	+	–
TMSMH-4	58.81	–	+	+	+	+	–
TMSMH-5	68.24	–	+	+	+	+	–
TMSMH-6	77.31	–	+	+	+	+	–

+: Almost soluble; –: Insoluble.

[a] Degree of substitution (DS) of maltoheptaose was measured as the average number of hydroxymethyl groups $-Si(CH_3)_3$ groups per all the –OH groups in the maltoheptaose, calculated for the intensity of I_{H1} and $I_{-Si(CH3)3}$ by ^{1}H NMR. $DS = 7I_{Si(Me_3)_3}/(23 * 9I_{H_1}) \times 100\%$.

[b] DMSO, dimethyl sulfoxide.

first heated from 25 to 100 °C at a rate of 10 °C/min (first scan), cooled to room temperature at a cooling rate of 10 °C/min, and then heated again to 100 °C at a rate of 10 °C/min (second scan). Wide-angle X-ray diffraction (WAXD) measurements were carried out on an X-ray diffractometer (MSAL XD-2, China) operating at 40 kV and 200 mA. Nickel-filtered Cu K_α radiation (λ = 0.154 nm) was used.

3. Results and discussion

3.1. Maltoheptaose from β-cyclodextrin

As shown in Scheme 1, the α-1,4 glucose bond of β-cyclodextrin (β-CD) is cleaved readily in an appropriate acidic solution, and the maltoheptaose (MH) contaminated only by traces of oligoglucans ($Glcz_6$ up to $Glcz_2$) can be achieved. Pure precipitated maltoheptaose is obtained by reprecipitation with water as solvent and ethanol as precipitant. β-cyclodextrin has poor solubility in water, but maltoheptaose (MH) is soluble in water. With the opening of the β-cyclodextrin (β-CD) ring, the cyclo-structure of β-cyclodextrin (β-CD) changed into a line chain, and two other –OHs can be observed. Obvious differences in the IR spectrum between maltoheptaose (MH) and β-cyclodextrin (β-CD) cannot be observed in Fig. 1. However, with the β-cyclodextrin (β-CD) ring opening, the *cis*- and *trans*-formation of glucose can be observed, and a new peak at 5.1 ppm can be found in the ^{1}H NMR spectrum (Fig. 2). Differences are also shown in the X-ray diffraction profiles (Fig. 3). β-cyclodextrin (β-CD) formed crystals, and the narrow peak at $2\theta = 9.14, 12.89, 14.92, 18.97$ was readily observed. However, maltoheptaose (MH) precipitated from ethanol is non-crystalline, and only the broad diffraction peck at $2\theta = 17.80$ can be found.

3.2. Maltoheptaose silylation reaction

The preparation of the MH-g-PCL copolymer was carried out according to the procedure shown in Scheme 1. Trimethylsilyl maltoheptaose (TMSMH) was synthesized from maltoheptaose and hexamethyldisilazane (HMDS) in DMSO solvent at 80 °C, in which the –OH group substituted by trimethylsilyl groups (defined as D_{TMS}) was controlled by the adjustment of the molar ratio of MH and HMDS.

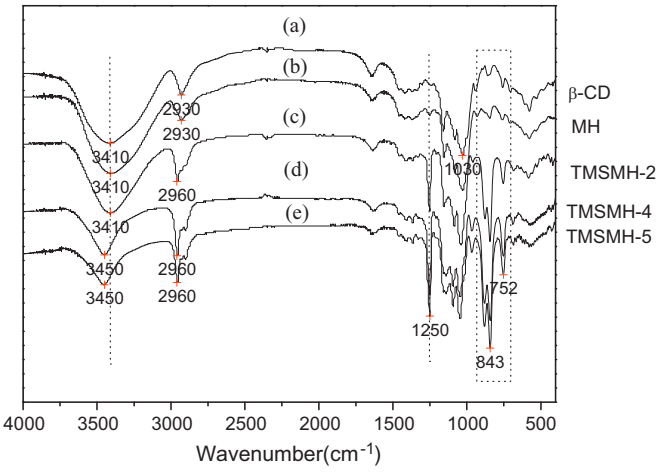

Fig. 1. FTIR spectra of β-CD, MH, and TMSMH with different D_{TMS}. (a) β-CD, (b) MH, (c) TMSMH-2, (d) TMSMH-4, and (e) TMSMH-5.

Comparing the spectra of TMSMH with maltoheptaose, a new peak in the region 1250 cm^{-1} and three new peaks in the region 891–748 cm^{-1}, all corresponding to the $Si–CH_3$ group, can be observed (Fig. 1). The signal at 1000–1100 cm^{-1} is due to both the CH_3–Si–O-maltoheptaose bond and the C–O–C bond of the maltoheptaose chain. An increase in D_{TMS} increases the relative stretching intensity of the $Si–CH_3$ group at 1250 cm^{-1}. The remaining peak around 3410–3450 cm^{-1} is attributed to the stretching vibration of the associated –OH group, indicating that maltoheptaose is not completely substituted. As shown in Fig. 1, the associated –OH frequency of TMSMH shifts upwards compared with that of MH, and the relative stretching intensity decreases with an increase in D_{TMS}, suggesting that the intermolecular and

Table 2
Characterization and thermal properties of MH-g-PCL copolymers.

Sample	Characterization		Thermal properties		
	DP of PCL[a]	M_n[b] (M_w/M_n[b])	First heating (10 °C/min) T_{m1} (°C)	First cooling (10 °C/min) T_c (°C)	Second heating (10 °C/min) T_{m2} (°C)
g_1 (MH_7-g-PCL_2)	2	–	61.73	39.21	55.40
g_2(MH_7-g-PCL_{10})	10	15,689 (1.64)	63.79	39.43	58.43
g_3(MH_7-g-PCL_{60})	60	30,903 (1.54)	63.86	40.05	58.75

MH-g-PCL with different length of PCL branches were denoted MH_7-g-PCL_x, wherein the suffix of 7 means the number of glucose unit of maltohepatoase, and the suffix of *x* means the polymerization degree of a single PCL branch attached to pyranose unit. DS of the TMSMH employed was 68.24%.

[a] Calculated by the result of ^{1}H NMR.

[b] Estimated by GPC in THF.

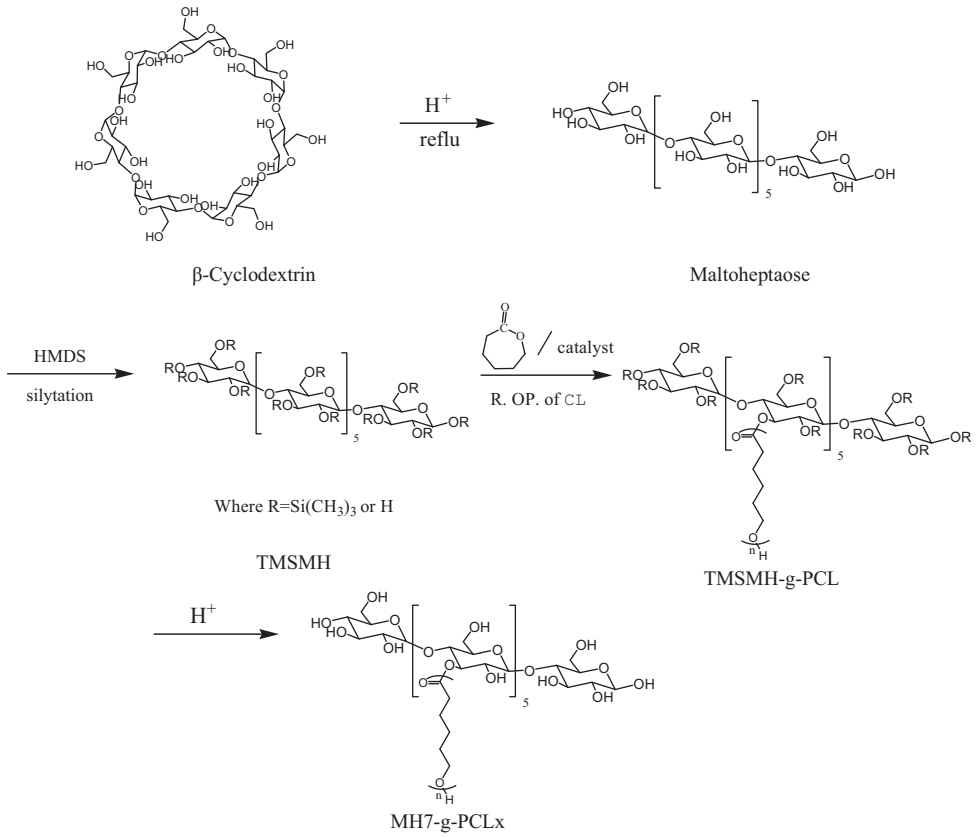

Scheme 1. Graft copolymerization of ε-caprolactone onto maltoheptaose.

intramolecular hydrogen bonding in TMSMH weakens with the loss of –OH groups.

The introduction of the TMS group was also confirmed from the methyl proton signal at $\delta = 0.1$ ppm in addition to the methylene protons (H-1) signal of the monosaccharide residue groups at $\delta = 5.0$ ppm and the broad methine and methylene proton signals of the parent maltoheptaose at $\delta = 3.0$–4.0 ppm in the ^{1}H NMR spectrum in $CDCl_3$ (Fig. 2). The D_{TMS} of TMSMH was determined from the ratio of the integral areas of the signals for the methyl protons of the TMS groups at $\delta = 0.1$ ppm to those for the methyl protons of the methylene protons (H-1) signal of the monosaccharide residue groups at $\delta = 5.0$ ppm. The D_{TMS} were all less than 3, indicating that the hydroxyl groups of MH were only partly substituted by the TMS groups. Table 1 shows the degree of substitution which were calculated by ^{1}H NMR spectrum.

As shown in Fig. 3, the broad peaks of MH and TMSMH reveal amorphous structures. The peaks around $2\theta = 8$–9° and $2\theta = 15$–17° indicate that the structural characteristics of linear oligosaccharide are preserved, with two peaks corresponding to the 101 and $10\bar{1}$ planes. However, comparisons of the pattern of TMSMH with that of the parent MH indicate broader peaks and smaller diffraction

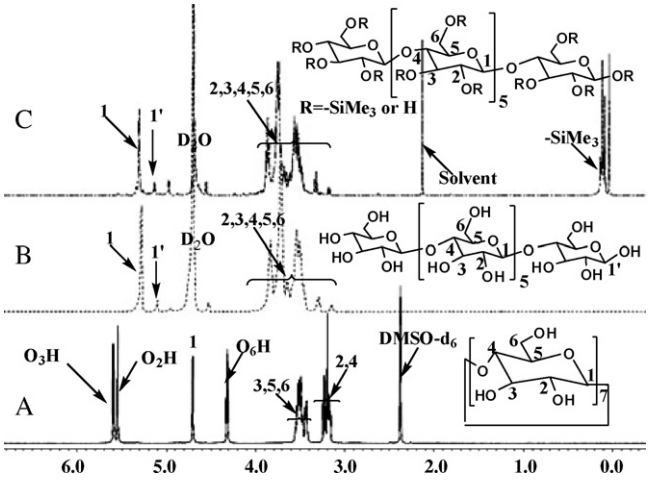

Fig. 2. ^{1}H NMR spectrum of (A) β-CD (in DMSO-d_6), (B) MH (in D_2O), and (C) TMSMH-1 (in D_2O).

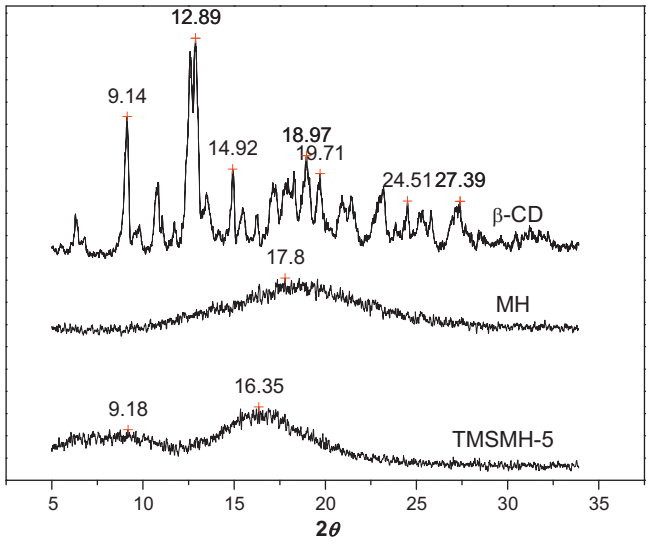

Fig. 3. X-ray diffraction profiles of (a) β-CD, (b) maltoheptaose (MH), and (c) TMSMH-5.

sample	DS(%)	M_n [c]	M_n [a]	M_w [a]	Polydispersity [a]
TMSMH-4	58.81	2127	2140	2259	1.05
TMSMH-5	68.24	2283	2249	2381	1.03

[c]Ccalculated by the results of 1H-NMR.
[a]Estimated by GPC in THF.

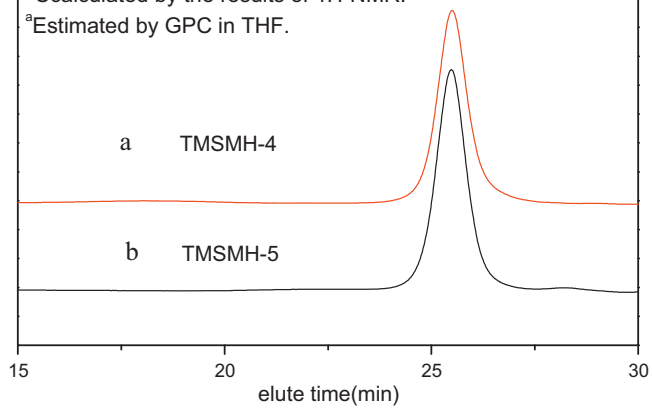

Fig. 4. GPC traces of the resultant silylated maltoheptaose with a different DS. (a) TMSMH-4 (DS = 58.81%) and (b) TMSMH-5 (DS = 68.24%).

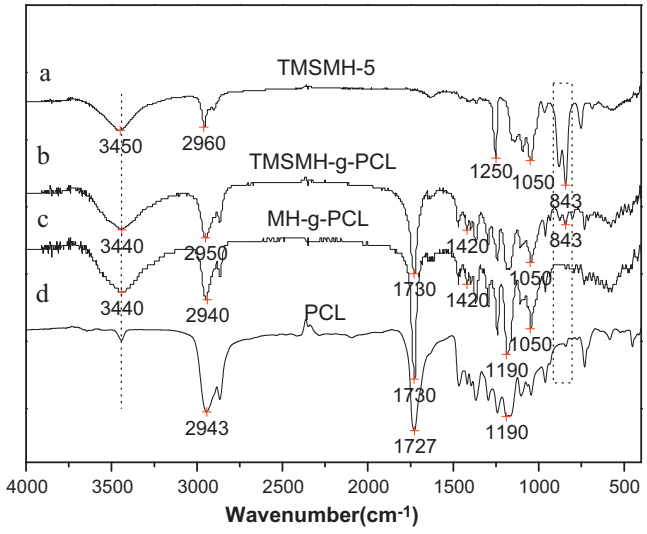

Fig. 5. IR spectra of (a) TMSMH-5, (b) TMSMH-g-PCL, (c) MH-g-PCL and (d) PCL.

angles corresponding to larger d_{101} and d_{101} values calculated by the Bragg equation (Fig. 3). Taking into account the previous discussion on the IR results, this can be attributed to not only the loss of the hydrogen bond but also the steric hindrance effect of the TMS groups after the hydroxyl group in the plane of 101 and $10\bar{1}$ was partially substituted by the TMS group.

As shown in Table 1, maltoheptaose (MH) dissolved only in water and some strong polar solvent (for example, DMSO and DMF). The obtained TMSMH achieved solubility in a variety of organic solvents, such as chloroform, acetone, THF and p-xylene. Insolubility in DMF and DMSO increased with the substitution of trimethylsilyl groups (D_{TMS} > 48.77%), indicating that the polarity of TMSMH decreases with an increase in D_{TMS}. Together with the previous discussion on the IR and WAXD results, the intermolecular and intramolecular hydrogen bond in the TMSMH weakens with the loss of –OH groups, and the structure of TMSMH becomes more expanded and disorganized compared with MH, all contributing to its easier dissolution in common organic solvent. As shown in Fig. 4, the molecular distributions (M_w/M_n) of TMSMH-4 (58.81%) and TMSMH-5 (68.24%) were around 1.0, proving that the maltoheptaose from β-cyclodextrin was monodispersed.

3.3. ROP of CL and deprotection of TMS-maltoheptaose-g-PCL

In the ROP of CL, the DS of TMSMH employed was approximately 68.24%. For this highly silylated MH, the glucose units were nearly disilylated with a majority of the remaining free hydroxyl groups in the third position (OH^3) due to the relative weak reactivity of the OH^3 group in each glucose unit toward silylation (Nouvel et al., 2004b). About 7 OH^3 groups per 7 glucose units remained, and these remaining free hydroxyl groups can serve as the initiating points for the subsequent ROP reaction of ε-caprolactone.

The obtained TMSMH achieved solubility in a variety of organic solvents. Therefore, the homogeneous ring-opening grafting copolymerization of ε-caprolactone onto the modified MH was successfully carried out in a non-polar p-xylene solvent.

Finally, the TMS protection groups of TMSMH-g-PCL were removed by the incubation of the polymer samples into an isopropyl alcohol/H_2O/HCl mixture. The disappearance of absorption bands related to the trimethylsilyl groups at 750, 843, 874, 1050, 1190, and 1250 cm^{-1} can be shown by FT-IR spectroscopy (Fig. 5). The ^1H NMR spectrum of TMS-deprotected MH-g-PCL was in good agreement with the expected structure as shown in Fig. 6. The deprotection of the TMS groups was confirmed by the disappearance of methyl proton signals from TMS at 0.10 ppm. The methylene proton signals of PCL can be observed at 4.1 ppm (three peaks), 2.3 ppm (three peaks), 1.7 ppm (multipeaks), and 1.4 ppm (multipeaks). The methine proton signal was at 4.3 ppm, and methylene proton signals were at 3.0–4.0 ppm.

The incorporation of TMS groups ensures the control of the PCL graft number and the position on the MH backbone. The average degree of ε-caprolactone grafted on every glucose unit of MH backbone (DP) was calculated from the ratio of the integrated area of the methylene signal of PCL at 2.3 ppm to the methine proton signal (H-1) of MH at 4.3 ppm (Table 2). The average length of every PCL number can be calculated by considering that the number of the remaining hydroxyl groups in every glucose unit is about 1 and assuming that the free remaining hydroxyl group of the partially silylated maltoheptaose (MH) can effectively initiate the ROP of CL.

As shown in Fig. 7, the contamination of the PCL homopolymer resulting from transesterification was not detected in the GPC curves. Furthermore, the molecular weight distribution is narrow ($1.54 \le M_w/M_n \le 1.64$).

In this work, MH has a molecular weight of 1152, which means that the amount of glucose units per MH chain is 7. The structure

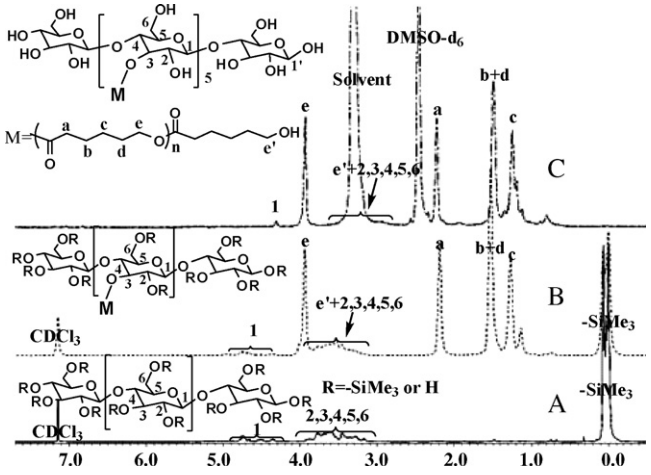

Fig. 6. ^1H NMR spectrum of (A) TMSMH-5 (in $CDCl_3$), (B) TMS-protected graft copolymer TMSMH-g-PCL (in $CDCl_3$), and (C)TMS-deprotected graft copolymer MH-g-PCL (in DMSO-d_6).

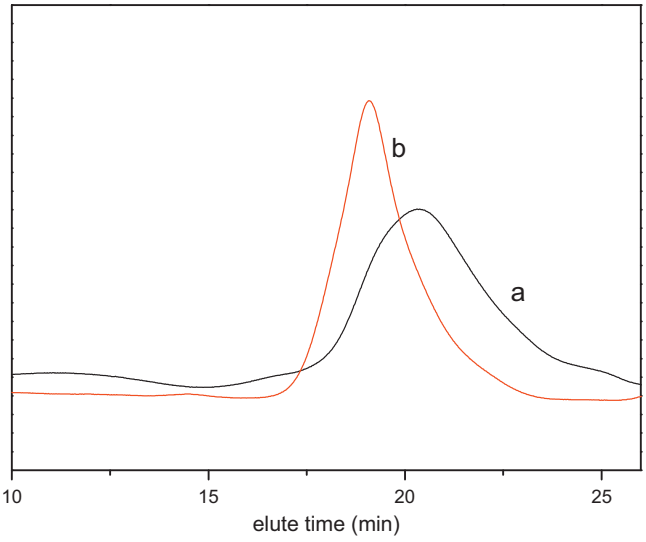

Fig. 7. GPC traces of poly(ε-caprolactone)-grafted maltoheptaose with different PCL lengths. (a) MH_7-g-PCL_{10}, and (b) MH_7-g-PCL_{60}.

of the obtained graft copolymer is comb shaped when the short oligo(ε-caprolactone) is grafted onto MH backbone. Increasing the length of ε-caprolactone segments transforms the structure of the obtained graft copolymer into brush shaped. It becomes tassel shaped with an asymmetric and unconventional graft copolymer structure consisting of a short main chain as backbone and long side chains as grafting segments. The schematic representations of their architecture are shown in Fig. 8.

3.4. Thermal analysis of MH-g-PCL copolymers

The crystalline property of amphiphilic copolymer influences its biodegradation and the hierarchical structure of its formed nanoparticles (Lin, & Gast, 1996; Portinha, Bouteiller, Pensec, & Richez, 2004; Richter, Schneiders, Monkenbusch, & Willner, 1997; Ohya et al., 1998). Thus, the thermal behavior of the synthesized new graft copolymers with a different D_p was investigated using DSC. PCL homopolymer is a semicrystalline polymer. The detected thermal phenomenon in DSC can only be attributed to PCL segments in MH-g-PCL because MH did not show any melting transition. The melting points of crystalline polymers may also depend on the thermal history of the sample. To erase the thermal history of the samples, the DSC thermograms were recorded during the second heating at 10 °C/min (Fig. 9). The values of the melting temperature (T_m) of all samples at first heating, first cooling, and second heating are listed in Table 2. The melting temperature(T_m) shifted from 55.4 °C to 58.4 °C with the increase

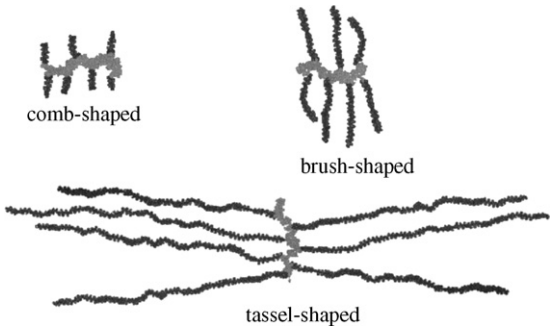

Fig. 8. Schematic illustration of comb-shaped, brush-shaped, and tassel-shaped copolymers with different branch lengths.

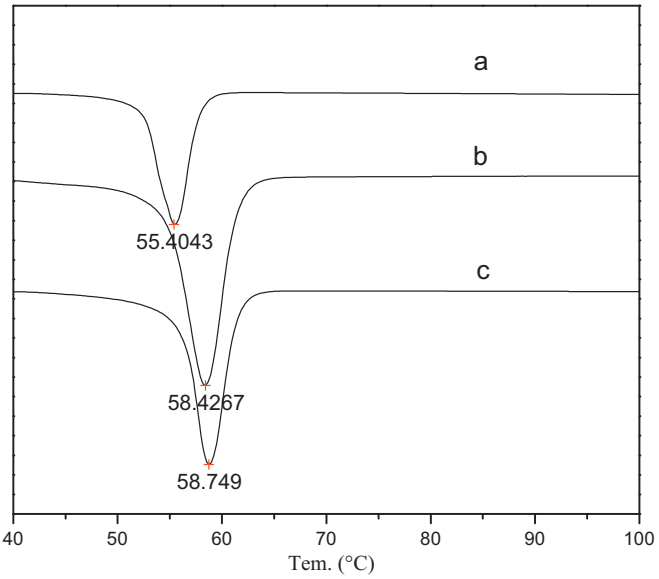

Fig. 9. DSC thermograms of (a) MH_7-g-PCL_2, (b) MH_7-g-PCL_{10}, and (c) MH_7-g-PCL_{60} with a rate of 10 °C/min at second heating run.

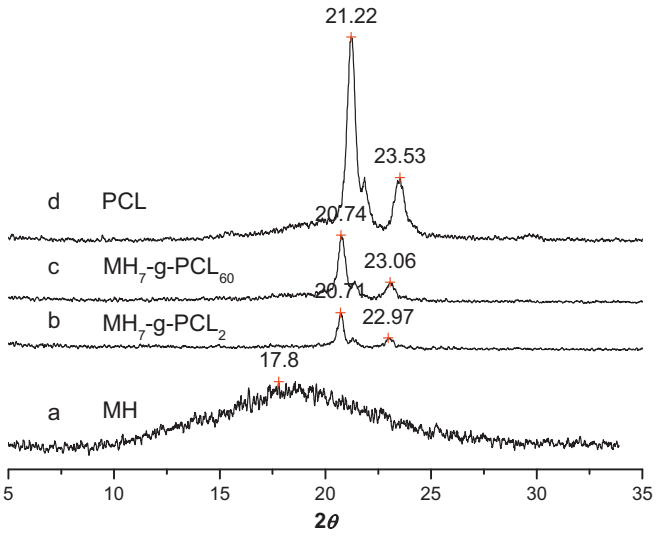

Fig. 10. X-ray diffraction profiles of (a) maltoheptaose (MH), (b) MH_7-g-PCL_2, (c) MH_7-g-PCL_{60}, and (d) PCL.

in side chain lengths of the copolymer from 2 to 10. However, the influence of the maltoheptaoses is weak that the continual increase in side chain length did not alter the crystallization and melting temperatures.

The results of the XRD analysis of the grafted copolymers are shown in Fig. 10. Compared with 10-a, a peak of the PCL segment in the grafting copolymers is observed, and the peak intensity of the PCL segments is increased with an increase in side chain length (Fig. 10b and c).

4. Conclusion

Amphiphilic graft copolymers (MH-g-PCL) with controlled structures were synthesized by protection and deprotection of the partial hydroxyl groups of MH via TMS groups and homogenous ring-opening polymerization of ε-caprolactone with stannous octoate as catalyst. A new kind of graft copolymers with controlled structure was obtained by adjusting the molar ratio of the CL to

MH glucose unit. Crystalline properties indicate that an increase in PCL content in the graft copolymer results in a higher T_m. The synthesis method can be applied to other oligosaccharides and biodegradable aliphatic polyesters, such as poly(lactone, lactide, and glycolide). Furthermore, such copolymers are expected to be applied as potential drug carrier materials.

Acknowledgment

This research was financially supported by the Natural Science Foundation of China (Grant No. 20604033)

References

Breitenkamp, K., & Emrick, T. (2003). Novel polymer capsules from amphiphilic graft copolymers and cross-metathesis. *Journal of American Chemical Society*, *125*(40), 12070–12071.

Caillol, S., Lecommandoux, S., Mingotaud, A.-F., Schappacher, M., Soum, A., Bryson, N., et al. (2003). Synthesis and self-assembly properties of peptide–polylactide block copolymers. *Macromolecules*, *36*(4), 1118–1124.

Chang, Y., Bender, J. D., Phelps, M. V. B., & Allcock, H. R. (2002). Synthesis and self-association behavior of biodegradable amphiphilic poly[bis (ethyl glycinat-n-yl)phosphazene]–poly(ethylene oxide) block copolymers. *Biomacromolecule*, *3*(6), 1364–1369.

Hua, Y., Jianga, X., Dinga, Y., Gea, H., Yuanb, Y., & Yanga, C. (2002). Synthesis and characterization of chitosan-poly (acrylic acid) nanoparticles. *Biomaterials*, *23*(15), 3193–3201.

Li, P., Zhu, J., Sunintaboon, P., & Harris, F. W. (2002). New route to amphiphilic core–shell polymer nanospheres: Graft copolymerization of methyl methacrylate from water-soluble polymer chains containing amino groups. *Langmuir*, *18*(22), 8641–8646.

Lin, E. K., & Gast, A. P. (1996). Semicrystalline diblock copolymer platelets in dilute solution. *Macromolecule*, *29*(12), 4432–4441.

Liu, Y., Tian, F., & Hu, K. A. (2004). Synthesis and characterization of a brush-like copolymer of polylactide grafted onto chitosan. *Carbohydrate Research*, *339*(4), 845–851.

Luo, L., Ranger, M., Lessard, D. G., Garrec, D. L., Gori, S., Leroux, J.-C., et al. (2004). Novel amphiphilic diblock copolymer of low molecular weight poly (*n*-vinylpyrrolidone)-block-poly (D,L-lactide): Synthesis, characterization, and micellization. *Macromolecules*, *37*(11), 4008–4013.

Jeong, J. H., Kang, H. S., Yang, S. R., & Kim, J.-D. (2002). Polymer micelle-like aggregates of novel amphiphilic biodegradable poly (asparagine) grafted with poly (caprolactone). *Polymer*, *44*(3), 583–591.

Nie, T., Zhao, Y., Xie, Z. W., & Wu, C. (2003). Micellar formation of poly (caprolactone-block-ethylene oxide-block-caprolactone) and its enzymatic biodegradation in aqueous dispersion. *Macromolecules*, *36*(23), 8825–8829.

Nouvel, C., Frochot, C., Sadtler, V., Dubois, P., Dellacherie, E., & Six, J.-L. (2004). Polylactide-grafted dextrans: Synthesis and properties at interfaces and in solution. *Macromolecules*, *37*(13), 4981–4988.

Nouvel, C., Dubois, P., Dellacherie, E., & Six, J.-L. (2004). Controlled synthesis of amphiphilic biodegradable polylactide-grafted dextran copolymers. *Journal of Polymer Science Part A: Polymer Chemistry*, *42*(11), 2577–2588.

Ouchi, Tatsuro, Kontani, Tomohiro, & Ohya, Yuichi. (2003). Mechanical property and biodegradability of solution-cast films prepared from amphiphilic polylactide-grafted dextran. *Journal of Polymer Science Part A: Polymer Chemistry*, *41*(16), 2462–2468.

Ohya, Yuichi, Maruhashi, Shotaro, & Ouchi, Tatsuro. (1998). Graft polymerization of L-lactide on pullulan through the trimethylsilyl protection method and degradation of the graft copolymers. *Macromolecules*, *31*(14), 4662–4665.

Portinha, D., Bouteiller, L., Pensec, S., & Richez, A. (2004). Influence of preparation conditions on the self-assembly by stereocomplexation of polylactide containing diblock copolymers. *Macromolecules*, *37*(9), 3401–3406.

Richter, D., Schneiders, D., Monkenbusch, M., & Willner, L. (1997). Polymer aggregates with crystalline cores: The system polyethylene–poly(ethylenepropylene). *Macromolecules*, *30*(4), 1053–1068.

Rosler, Annette, Vandermeulen, Guido W. M., & Klok, Harm-Anton. (2001). Advanced drug delivery devices via self-assembly of amphiphilic block copolymers. *Advanced Drug Delivery Reviews*, *53*(1), 95–108.

Sato, Y., Kobayashi, Y., Kamiya, T., Watanabe, H., Akaike, T., Yoshikawa, K., et al. (2005). The effect of backbone structure on polycation comb-type copolymer/DNA interactions and the molecular assembly of DNA. *Biomaterials*, *26*(7), 703–711.

Tatsuro, O., Tomohiro, K., & Yuichi, O. (2003). Mechanical property and biodegradability of solution-cast films prepared from amphiphilic polylactide-grafted dextran. *Journal of Polymer Science Part A: Polymer Chemistry*, *41*(16), 2462–2468.

Volker, v. B., Gerd, J., & Reimund, S. (1995). Enzymatic grafting of amylose from poly (dimethylsi1oxanes). *Macromolecules*, *28*, 17–24.

Wang, C. Q., Dong, Y. P., & Tan, H. M. (2003). Biodegradable brushlike graft polymers. I. polymerization of caprolactone onto water-soluble hydroxypropyl cellulose as the backbone by the protection of the trimethylsilyl group. *Journal of Polymer Science: Part A: Polymer Chemistry*, *41*, 273–280.

Wang, C., Li, G., & Guo, R. (2005). Multiple morphologies from amphiphilic graft copolymers based on chitooligosaccharides as backbones and polycaprolactones as branches. *Chemical Communications*, 3591–3593.

Xiong, X. Y., Tam, K. C., & Gan, L. H. (2003). Synthesis and aggregation behavior of pluronic f127/poly (lactic acid) block copolymers in aqueous solutions. *Macromolecules*, *36*(26), 9979–9985.

Yao, F., Liu, C., Chen, W., Bai, Y., Tang, Z., & Yao, K. (2003). Synthesis and characterization of chitosan grafted oligo (L-lactic acid). *Macromolecular Bioscience*, *3*(11), 653–656.

Ydens, I., Rutot, D., Degee, P., Six, J.-L., Dellacherie, E., & Dubois, P. (2000). Controlled synthesis of poly (ε-caprolactone)-grafted dextran copolymers as potential environmentally friendly surfactants. *Macromolecules*, *33*(18), 6713–6721.